Supporting Information for

The Irony of Manganocene – An Interplay Between the Jahn-Teller Effect and Close Lying Electronic and Spin States

Stepan Stepanović[1], Matija Zlatar[1], Marcel Swart[2,3], Maja Gruden[4*]

[1]Department of Chemistry, Institute of Chemistry, Technology and Metallurgy, University of Belgrade, Studentski trg 12-16, Belgrade, Serbia

[2]Institut de Química Computacional i Catàlisi (IQCC) and Departament de Química, Universitat de Girona, Campus Montilivi, Facultat de Ciències, 17003 Girona, Spain

[3]ICREA, Pg. Lluís Companys 23, 08010 Barcelona, Spain

[4] University of Belgrade - Faculty of Chemistry, Studentski trg 12-16, Belgrade, Serbia

Corresponding Author

*E-mail: gmaja@chem.bg.ac.rs

Table of Contents

Theoretical background and Computational details

All DFT calculations were performed with the Amsterdam Density Functional (ADF) suite of program.[1,2] MOs were expanded in an uncontracted set of Slater type orbitals (STOs) of triple-ζ quality (TZP)[3] and one set of polarization functions. An auxiliary set of s, p, d, f, and g STOs was used to fit the molecular density and to represent the Coulomb and exchange potentials accurately for each SCF cycle.
 Geometries were optimized with the QUILD program[4] using adapted delocalized coordinates[5] until the maximum gradient component was less than 10^{-4} a.u. Energies and gradients were calculated using the OPBE level of theory.[6,7] Nature of stationary points is confirmed by calculating analytical Hessians.

If any nonlinear molecule is found in the electronically degenerate state, there exist a non-totally symmetric normal mode which can reduce the symmetry, remove the degeneracy and lower the energy. In many real-life Jahn-Teller problems, there is more than one normal mode that participates in the structural relaxation and this situation is referred to as a multimode problem. The non-totally symmetric normal mode will distort the geometry to the first subgroup in which at least one of its components belongs to the total symmetric irreducible representation (irrep.). That JT active normal mode may not be the only symmetry label from the high symmetry point group that becomes total symmetric in the new point group and the contributions from all these modes are successfully captured using IDP methodology. In this Manuscript, the high symmetry point groups are D_{5h} and D_{5d}, the JT active normal mode belongs to the E_1' and E_{1g} irreps., and they distort the structure to the C_{2v} and C_{2h} point groups, respectively.

Degenerate states were treated in accordance with all our previous work regarding Jahn-Teller effect,[8-11] by optimizing the geometry with a high symmetry structural constraint and AOC electronic configuration (with E_2' state of manganocene, that would mean $(e_2')^3(a_1')^2(e_1'')$ electronic configuration, in which ADF occupies the degenerate e_2' orbitals with 0.5 β electrons each). Using this structure, the subsequent single points have been performed with the electronic density relaxed to a low symmetry subgroup (for D_{5h} the first subgroup is C_{2v}: $e_2' \rightarrow a_1 + b_1$; $a_1' \rightarrow a_1$; $e_1'' \rightarrow a_2 + b_2$), with the two possible resulting configurations:

$(e_2')^3(a_1')^2(e_1'') \rightarrow (a_1)^2(b_2)^1(a_1)^2(a_2)(b_1)$ or $(a_1)^1(b_2)^2(a_1)^2(a_2)(b_1)$.
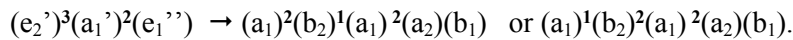
Detailed descriptions of IDP and Jahn-Teller effect are presented elsewhere.[9-11] **The essence of the IDP is** to express the distortion along a model minimal energy path, projecting the one nuclear configuration to the normal modes of the other. This allows to determine the presence and significance of all normal modes involved. Normal modes are labeled with Q_i, and E_{JT} represents energy difference between high symmetry and low symmetry structures, whereas R_{JT} is used to describe the corresponding geometrical distortion. Analytical frequencies were calculated with ADF2013, OPBE/TZP/integration 6 level of theory, on AOC electronic configurations in degenerate states. In D_{5h} geometry, since the symmetry of the degenerate electronic state is E'_2 the JT active vibrations must belong to E'_1 irreducible representation. For the distortion in manganocene and ferrocenyl cation from $D_{5h} \rightarrow C_{2v}$ geometry, the projection of the JT distortion on the normal modes (Eq. 1) of both low symmetry (in eq. LS) and high symmetry (in eq. HS) is compared:

$$R_{JT} = \sum_i \omega_i^{LS(HS)} \cdot Q_i^{LS(HS)} \xrightarrow{\text{normalizing } \omega_i^{LS(HS)} \text{ to 1}} C_i^{LS(HS)} \text{ with } \sum_i \left(C_i^{LS(HS)}\right)^2 = 1 \qquad \text{Eq. 1}$$

Coefficients $\omega_i^{LS(HS)}$ give a contribution of certain normal mode to the JT distortion, and they can be expressed in normalized form as $C_i^{LS(HS)}$. $E_i^{LS(HS)}$ and $F_i^{LS(HS)}$ show contributions through the specific normal modes to the E_{JT} and force at high symmetry point.

The energy of the nuclear configuration E_X, relative to the energy of the reference low symmetry configuration, in harmonic approximation, is expressed as the sum of the energy contributions of all low symmetry totally symmetric normal coordinates (N_{a1}):

$$E_X = \sum_{k=1}^{N_{a1}} E_{kX} = \frac{1}{2} \sum_{k=1}^{N_{a1}} w_{Xk}{}^2 \vec{Q}_k{}^2 \lambda_k \qquad \text{Eq.2}$$

where λ_k are the eigenvalues of the Hessian from the DFT calculations in the low symmetry minimum energy conformation. In this framework, we can analyze the multimode JT problem by expressing the R_{JT} as a superposition of all of the totally symmetric normal coordinates and directly obtaining the energy contributions of all of the normal modes to the total stabilization energy:

$$E_{JT} = \sum_{k=1}^{N_{a1}} E_{kJT} = \frac{1}{2} \sum_{k=1}^{N_{a1}} w_{kJT}{}^2 \vec{Q}_k{}^2 \lambda_k \qquad \text{Eq.3}$$

The force along the normal mode Q_k, F_{Xk}, which drives the nuclei along that coordinate to the minimum, at any point is defined as a derivative of the energy over the Cartesian coordinates.

$$\vec{F}_{Xtot} = \sum_{k=1}^{N_{a1}} \vec{F}_{Xk} = \frac{1}{2} \sum_{k=1}^{N_{a1}} w_{Xk} \lambda_k M^{1/2} \vec{Q}_k \qquad \text{Eq.4}$$

In the high symmetry point this will give information about the main driving force for the JT distortion.

All EDA calculations were performed with OPBE/TZ2P in order to minimize the basis set superposition error.

The magnetic behavior of coupled, spatially separated, local spins is commonly modeled using phenomenological Heisenberg-Dirac Hamiltonian,[12] that reduces complicated quantum mechanical problem to a simplified description in terms of spin degrees of freedom only. For a system that consist of two metal (or radical) centers it can be written as:

$\hat{H} = -J_{AB}\hat{S}_A \cdot \hat{S}_B$ where $\hat{S}_A$ and $\hat{S}_B$ are spin-operators associated with the spin-moments of unpaired electrons residing on spin-centers A and B. Only the total spin is physical observable, and in the case of two local spins, the possible total spins are given by Clebsch-Gordan Series: $S_A + S_B, S_A + S_B - 1, ... , |S_A - S_B|$. The two spin-centers are described as ferromagnetically aligned when they produce the maximum total spin $(S_A^\uparrow, S_B^\uparrow)$, and antiferromagnetically aligned when they produce minimum total spin $(S_A^\uparrow, S_B^\downarrow)$. The J_{AB} is the magnetic coupling parameter, which measures the strength of isotropic exchange interaction (is positive for ferromagnetic and negative for antiferromagnetic alignment). Thus, by knowing J_{AB}, it is possible to qualitatively account for the observed magnetic properties of the system. Currently the standard method for determining J_{AB} is by mapping differences in calculated total energies from electronic structure calculations onto the spin-states of Heisenberg-Dirac Hamiltonian [13]

The problem arises from the fact that only the ferromagnetically coupled ($S_{MAX} = S_A + S_B$) state can be properly described by one Slater determinant. This instantly leads to the conclusion that multideterminantal methodologies that are based on configuration interaction,[14,15] should be used. Unfortunately, such methodologies are usually too computationally demanding to study the large di- and poly nuclear TM complexes, or even the relatively small systems with many unpaired electrons are currently unfeasible.[12] Another drawback is the fact that these systems often possess considerable dynamical correlation, which makes the accurate calculations even more difficult.

Noodleman's suggestion[16,17] was the approach called the broken-symmetry (BS), that represent multideterminantal states with only one antiferromagnetically coupled Slater determinant. One of the artifacts that comes as a consequence of this is the appearance of spin density on sites A and B, although the real singlet state should have spin density equal to zero in any point.[18,19] The key step of the methodology is that orbitals are allowed to relax from the starting form under the action of the variational principle.[12,20] Thus, system is given the additional variational flexibility to lower its energy, and the ground state is formed variationally as a mixture of ferromagnetic state and singlet stats generated by charge-transfer (ionic states).[12,20] Although this process is essentially similar to CI, the BS formalism does not have enough flexibility and it can only mix single determinant ferromagnetic and ionic states, and the real ground state, multideterminantal singlet, is not included in a final result. Qualitatively, BS method yields a correct charge density, but, as previously mentioned, there is a fictitious spin density.[18,19]
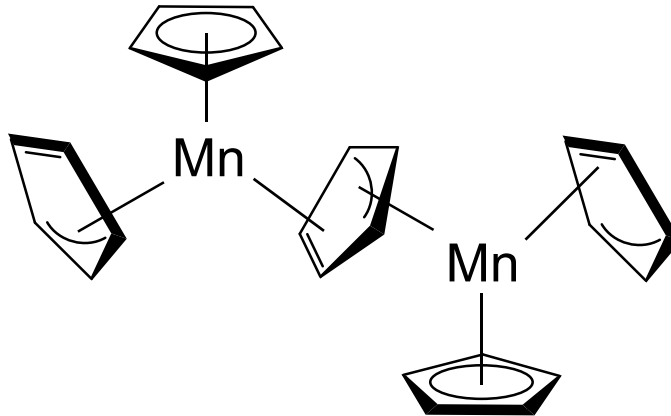
Scheme S1. Model for the manganocene dimer that was utilized to extract J_{AB} coupling constant.

We extracted J_{AB} by using the broken symmetry computational methodology that is s approximately valid over the entire coupling strength regime[21] (Eq. 4) and a dimer model shown on a Scheme S1.

$$J_{AB} = -\frac{E_{HS} - E_{BS}}{\langle S^2 \rangle_{HS} - \langle S^2 \rangle_{BS}} = -\frac{388.8 cm^{-1}}{30.04 - 5.01} = -15.5 cm^{-1} \qquad \text{Eq.4}$$

The coordinates for the utilized model are extracted from the X-ray structure of zigzag polymer.

$$\overline{e_1''} \qquad \overline{e_1''}$$

$$\overline{a_1'}$$

$$\overline{e_2'} \qquad \overline{e_2'}$$
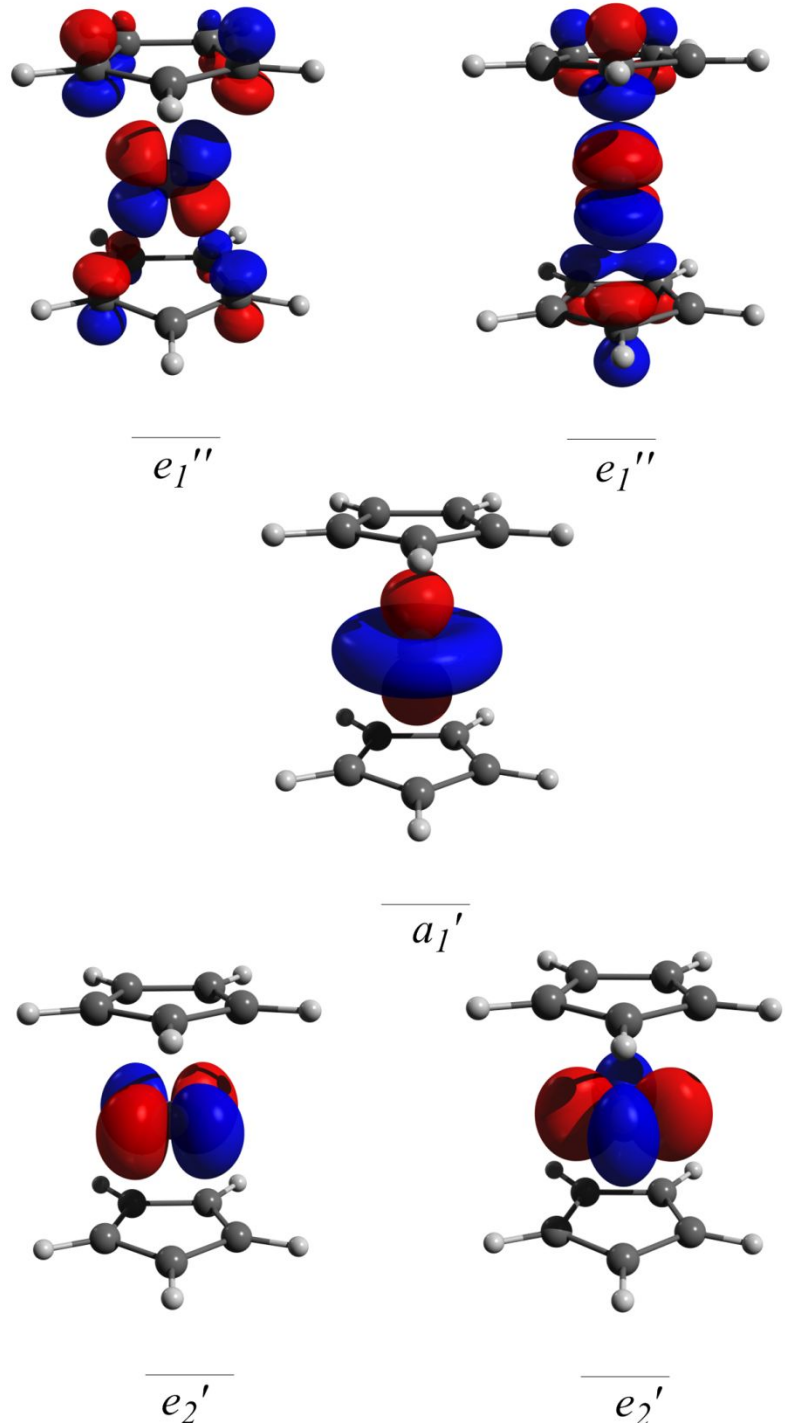
Figure S1. Frontier molecular orbitals for MnCp$_2$ in D$_{5h}$ symmetry.

Table S1. Selected average bond lengths (Å) for OPBE energy-minimized $MnCp_2$ structure and comparison to available gas phase diffraction data at elevated temperatures.

Distance(Å)	OPBE		Exp.[22]
	$^6A_1'$ (D_{5h})	$^2A_1$ (C_{2v})	
Mn-Cp	2.06	1.69	2.05
Mn-C	2.39	2.08	2.38
C-C	1.42	1.43	1.43
C-H	1.09	1.09	1.12

The EDA - results

As it can be noted from Table 1, with $Mn(Cp)_3$, interaction between prepared Mn^{2+} and $3Cp^{2-}$ fragments is greater for LS, but it is more than compensated with the ΔE_{prep}, specifically ΔE_{valexc} and $\Delta E_{cyc-cyc}$. Since ΔE_{valexc} is fairly constant for a given metal in the concrete oxidation state, only $\Delta E_{cyc-cyc}$ remains for the analysis. So, we conclude that the energy needed to bring $3Cp^-$ anions to a molecular geometry is much greater for more compact LS. As a conclusion we could state that unfavorable repulsion between the negative Cp^- anions overrides the stronger Ligands-Metal interactions in low spin state.

Table 2 shows similar trends with the important difference that repulsion between the negative Cp- anions in much smaller now and in is not enough to override the factors that stabilize the LS state.

The IDP analysis - results
The results of IDP analysis for $D_{5h} \rightarrow C_{2v}$ distortion are summarized in Table S2 (for decomposition in low symmetry normal modes), Table S3 (in high symmetry normal modes), and graphically presented in Fig. S2 and Fig. S3 respectively. For $D_{5d} \rightarrow C_{2h}$ distortion results are summarized in Table S4 (in high symmetry normal modes).

Table S2. Contributions of all low symmetry vibrations to the JT distortion $\left(C_i^{LS}\right)^2$, E_{JT} and force at high symmetry point.

|	Manganocene					Ferocenyl cation			
irrep	freq(cm⁻¹)	C_i^{LS}	E_i^{LS}(cm⁻¹)	F_i^{LS}(mdyne)	irrep	freq(cm⁻¹)	C_i^{LS}	E_i^{LS}(cm⁻¹)	F_i^{LS}(mdyne)
B2	-82.6	0	0	0	B2	-115.2	0	0	0
A2	45.7	0	0	0	A2	28.2	0	0	0
A1	**136.7**	**0.6161**	**55.344**	**-0.0158**	**A1**	**154.4**	**0.5931**	**62.5643**	**-0.0155**
A1	264.7	0.0086	2.9096	-0.0196	B2	216.5	0	0	0
B2	268	0	0	0	A1	301.6	0	0.0199	-0.0065
B1	363	0	0	0	B1	355.7	0	0	0
A2	369.4	0	0	0	A2	360	0	0	0
A1	**429.9**	**0.2966**	**263.502**	**0.182**	**A1**	**444.9**	**0.3963**	**347.0618**	**0.1989**
B1	477.4	0	0	0	B1	500.4	0	0	0
A1	581.5	0.0022	3.6517	0.0443	A1	550.5	0.0025	3.3276	-0.0191
B2	584	0	0	0	B1	568	0	0	0
A2	584.1	0	0	0	A2	576.4	0	0	0
B1	584.7	0	0	0	B2	584.6	0	0	0
A2	767.7	0	0	0	A1	703.1	0.0005	1.0205	-0.0139
B2	775	0	0	0	A2	800.5	0	0	0
B1	777.7	0	0	0	B1	807.1	0	0	0
A1	**784.9**	**0.0302**	**89.5715**	**-0.1077**	B2	827.7	0	0	0
A2	789.7	0	0	0	B1	848.7	0	0	0
B1	790.6	0	0	0	A1	849.1	0.0003	0.9153	-0.0109
A1	807.5	0.0011	3.3458	-0.0189	A2	852.7	0	0	0
B2	814.3	0	0	0	B1	857.9	0	0	0
B1	818.8	0	0	0	B2	861.8	0	0	0
A1	**827.6**	**0.0286**	**94.07**	**-0.1138**	A1	878.3	0.0046	15.5735	-0.0412
A2	847.6	0	0	0	A1	899.6	0.0006	2.1261	-0.0136
B2	855.2	0	0	0	A2	912.3	0	0	0
A1	868.6	0.0102	37.091	-0.0184	B2	916	0	0	0
B1	874.2	0	0	0	B1	929.1	0	0	0
B1	994.8	0	0	0	B2	1010.2	0	0	0
A1	1000.2	0.0037	17.6183	0.0357	A2	1013.4	0	0	0
A2	1001.7	0	0	0	B1	1014.6	0	0	0
B2	1002.3	0	0	0	A1	1019	0.0014	6.4918	-0.0225
B1	1041.4	0	0	0	A1	1037.6	0.0003	1.6519	-0.0146
A1	1043	0.0017	8.8368	0.0321	B1	1055.1	0	0	0
A2	1051.3	0	0	0	A2	1061.7	0	0	0
B2	1053.8	0	0	0	B2	1073.7	0	0	0
A1	1116.6	0.0004	2.179	-0.0355	A1	1131.3	0	0.0111	-0.0016
B1	1121.1	0	0	0	B1	1132.5	0	0	0
A2	1228.6	0	0	0	A2	1240.1	0	0	0
B2	1229.1	0	0	0	B2	1241.2	0	0	0
B1	1362.3	0	0	0	B1	1364.3	0	0	0
A1	1374.6	0.0001	0.7723	-0.01	A2	1377.9	0	0	0
A2	1380.4	0	0	0	A1	1383.6	0	0.0512	-0.0033
B2	1389.4	0	0	0	B2	1397.5	0	0	0
A1	1413.5	0.0005	4.9981	0.0655	B2	1426.5	0	0	0
B1	1414.7	0	0	0	A1	1432.2	0.0004	3.7575	-0.0576
B2	1424.1	0	0	0	B1	1433	0	0	0
A2	1426.7	0	0	0	A2	1433.1	0	0	0
B1	3167.5	0	0	0	A1	3193.7	0	0.0364	-0.0054
A1	3168.5	0	0.3706	0.0328	B1	3197.7	0	0	0
A2	3175.4	0	0	0	A2	3202.8	0	0	0
B2	3176	0	0	0	B2	3204.5	0	0	0
B1	3189	0	0	0	B1	3215	0	0	0
A1	3189.5	0	0.139	0.0047	A1	3216	0	0.0745	0.0088
A2	3195.2	0	0	0	A2	3216.3	0	0	0
B2	3195.4	0	0	0	B2	3217	0	0	0
A1	3203.1	0	0.1232	0.0188	B1	3229.2	0	0	0
B1	3205.5	0	0	0	A1	3229.9	0	0.0001	-0.0022
R_{JT}((amu) $^{1/2}$·Angst)=0.5694			E_{JT}(cm⁻¹)=584.5231			R_{JT}=0.5463		E_{JT}(cm⁻¹)=444.6834	
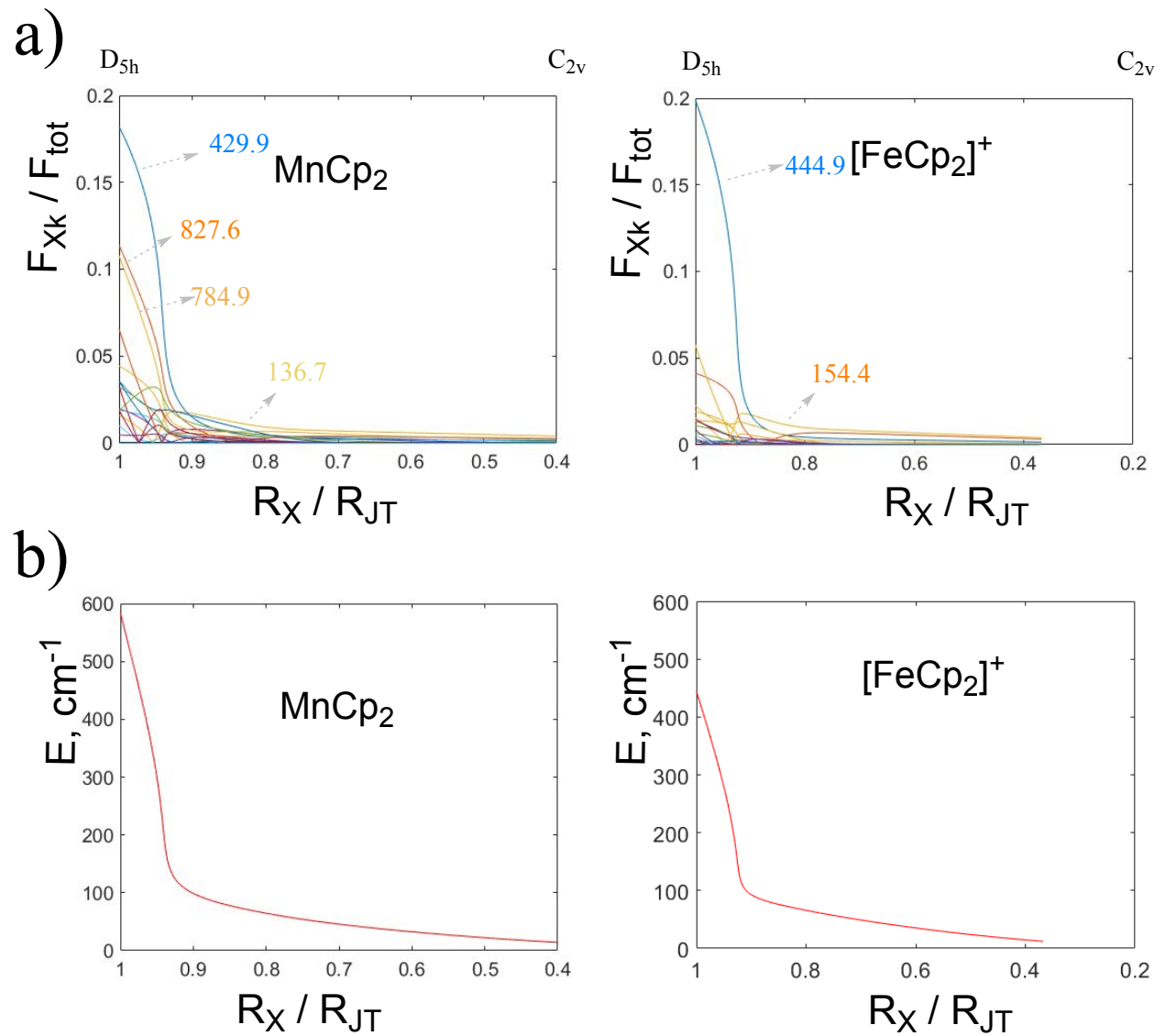
Figure S2. IDP analysis of low symmetry vibrations for both MnCp$_2$ and [FeCp$_2$]$^+$.

Table S3. Contributions of all high symmetry vibrations to the JT distortion $\left(C_i^{HS}\right)^2$, E_{JT} and force at high symmetry point.

Manganocene				Ferocenyl cation			
irrep	freq(cm⁻¹)	C_i^{HS}	$F_i^{HS}(mdyne)$	irrep	freq(cm⁻¹)	C_i^{HS}	$F_i^{HS}(mdyne)$
AAA1	38.9	0	0	AAA1	33.5	0	0
EE1:1	148.2	0	0	EE1:1	162.3	0	0
EE1:2	**148.2**	**0.6549**	**-0.0099**	**EE1:2**	**162.3**	**0.5780**	**0.0148**
AA1	298	0.0378	0.0244	AA1	304.8	0	-0.0029
EEE1:1	377.6	0	0	EEE1:1	369.5	0	0
EEE1:2	377.6	0	0	EEE1:2	369.5	0	0
AAA2	482.3	0	0	EE1:1	461.2	0	0
EE1:1	503.9	0	-0.0569	**EE1:2**	**461.2**	**0.3830**	**-0.2016**
EE1:2	**503.9**	**0.2543**	**-0.1958**	AAA2	503.6	0	0
EEE2:1	614	0	0	EEE2:1	592.6	0	0
EEE2:2	614	0	0	EEE2:2	592.6	0	0
EE2:1	626.5	0	0	EE2:1	610	0	0
EE2:2	626.5	0.0080	0.0572	EE2:2	610	0.0017	-0.0006
EEE1:1	786.2	0	0	EEE2:1	804.4	0	0
EEE1:2	786.2	0	0	EEE2:2	804.4	0	0
EEE2:1	793.2	0	0	EE2:1	831.3	0.0003	0.0037
EEE2:2	793.2	0	0	EE2:2	831.3	0	0
AAA2	805.1	0	0	AA1	852.5	0.0005	-0.0008
AA1	814.9	0.0004	0.0019	EEE1:1	854.5	0	0
EE2:1	823.7	0	0	EEE1:2	854.5	0	0
EE2:2	**823.7**	**0.0280**	**0.1169**	AAA2	856.8	0	0
EE1:1	826.7	0	0	EE1:1	881.2	0	0
EE1:2	826.7	0.0045	0.0350	EE1:2	881.2	0.0043	0.0406
EEE2:1	865.6	0	0	EEE2:1	924.6	0	0
EEE2:2	865.6	0	0	EEE2:2	924.6	0	0
EE2:1	880.4	0	0	EE2:1	932.5	0	0.0035
EE2:2	880.4	0.0044	-0.0077	EE2:2	932.5	0	0
EEE1:1	1002.1	0	0	EEE1:1	1016.3	0	0
EEE1:2	1002.1	0	0	EEE1:2	1016.3	0	0
EE1:1	1012.1	0.0034	0.0317	EE1:1	1022	0.0018	0.0262
EE1:2	1012.1	0	0	EE1:2	1022	0	0
EEE2:1	1048.6	0	0	EEE2:1	1059.5	0	0
EEE2:2	1048.6	0	0	EEE2:2	1059.5	0	0
EE2:1	1056	0.0031	0.0313	EE2:1	1072.5	0	0
EE2:2	1056	0	0	EE2:2	1072.5	0.0001	-0.0043
AAA2	1126.5	0	0	AA1	1134.2	0.0002	0.0026
AA1	1129.2	0	0.0416	AAA2	1134.6	0	0
AAA1	1232.2	0	0	AAA1	1242	0	0
AA2	1233	0	0	AA2	1243.2	0	0.0001
EEE2:1	1388.7	0	0	EEE2:1	1381.9	0	0
EEE2:2	1388.7	0	0	EEE2:2	1381.9	0	0
EE2:1	1405.4	0	0	EE2:1	1407.6	0	-0.0156
EE2:2	1405.4	0.0002	-0.0285	EE2:2	1407.6	0	0
EEE1:1	1424	0	0	EE1:1	1433.1	0	0
EEE1:2	1424	0	0	EE1:2	1433.1	0.0005	-0.0549
EE1:1	1425.9	0	0	EEE1:1	1435.1	0	0
EE1:2	1425.9	0.0010	-0.0632	EEE1:2	1435.1	0	0
EEE2:1	3171.2	0	0	EEE2:1	3199.4	0	0
EEE2:2	3171.2	0	0	EEE2:2	3199.4	0	0
EE2:1	3172.2	0	-0.0318	EE2:1	3201.1	0	0
EE2:2	3172.2	0	0	EE2:2	3201.1	0	-0.0046
EEE1:1	3188.4	0	0	EEE1:1	3214.4	0	0
EEE1:2	3188.4	0	0	EEE1:2	3214.4	0	0
EE1:1	3189.1	0	0	EE1:1	3215.5	0	0
EE1:2	3189.1	0	-0.0170	EE1:2	3215.5	0	-0.0100
AAA2	3201.9	0	0	AAA2	3227.6	0	0
AA1	3202.8	0	0.0144	AA1	3228.3	0	0.0004
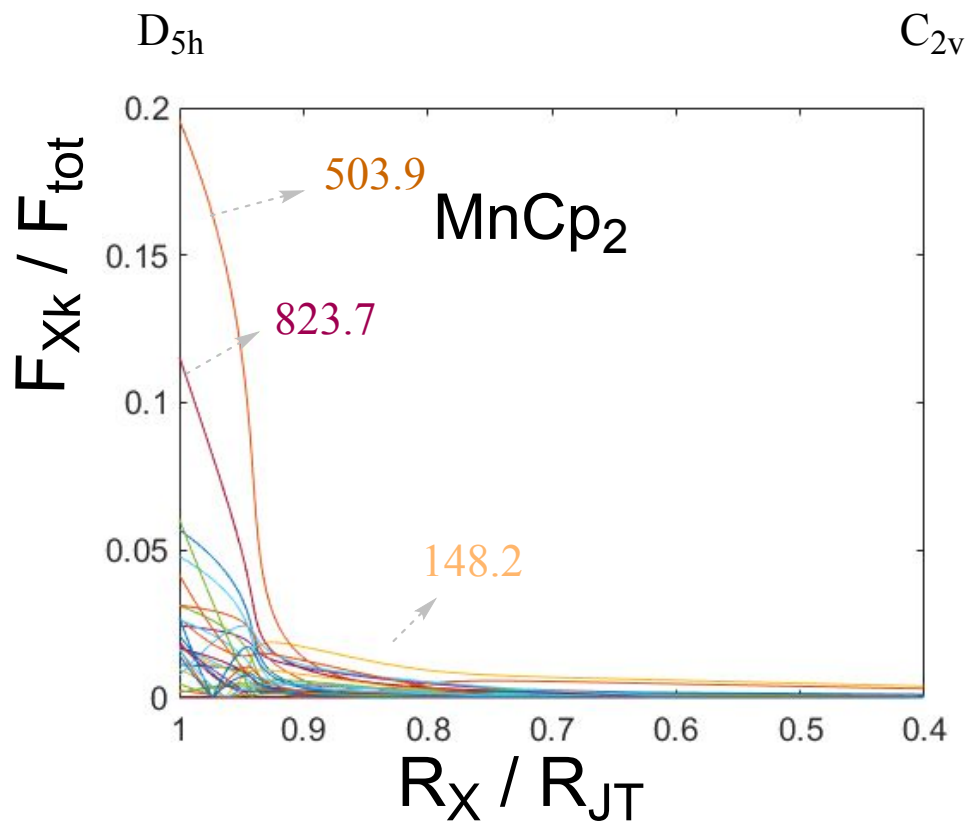
Figure S3. IDP analysis of the high symmetry vibrations in MnCp$_2$.

Table S4. Contributions of all high symmetry vibrations to the JT distortion $\left(C_i^{HS}\right)^2$, E_{JT} and force at high symmetry point (D5d).

	Ferocenyl cation				Manganocene		
freq(cm⁻¹)	irrep	C_i^{HS}	$F_i^{HS}(mdyne)$	freq(cm⁻¹)	irrep	C_i^{HS}	$F_i^{HS}(mdyne)$
12.3	A1.u	0	0	-22.3	A1.u	0	0
163.1	E1.u:1	0	0	151.1	E1.u:1	0	0
163.1	E1.u:2	0	0	151.1	E1.u:2	0	0
309.2	A1.g	0.0152	0.011	300.3	A1.g	0.0586	0.0172
378.4	E1.g:1	0.9643	0.1122	389	E1.g:1	0.8260	0.1096
378.4	E1.g:2	0	0	389	E1.g:2	0	0.021
452.1	E1.u:1	0	0	477.7	A2.u	0	0
452.1	E1.u:2	0	0	478.5	E1.u:1	0	0
507	A2.u	0	0	478.5	E1.u:2	0	0
589.7	E2.u:1	0	0	607.3	E2.u:1	0	0
589.7	E2.u:2	0	0	607.3	E2.u:2	0	0
613.4	E2.g:1	0	0	630.2	E2.g:1	0.0184	0.0601
613.4	E2.g:2	0.0005	0.0081	630.2	E2.g:2	0	0
802.5	E2.u:1	0	0	788.4	E1.g:1	0.0194	0.0615
802.5	E2.u:2	0	0	788.4	E1.g:2	0	0
833.5	E2.g:1	0	0.0022	792.3	E2.u:1	0	0
833.5	E2.g:2	0	0	792.3	E2.u:2	0	0
851.1	A1.g	0	0.0074	802.8	A2.u	0	0
854.2	E1.g:1	0.0146	0.0599	812.7	A1.g	0.0005	-0.0011
854.2	E1.g:2	0	0.0011	823.9	E2.g:1	0.0527	-0.1204
856.5	A2.u	0	0	823.9	E2.g:2	0	0
880.8	E1.u:1	0	0	824	E1.u:1	0	0
880.8	E1.u:2	0	0	824	E1.u:2	0	0
927	E2.g:1	0	-0.0038	867.4	E2.u:1	0	0
927	E2.g:2	0	0	867.4	E2.u:2	0	0
927.9	E2.u:1	0	0	876.6	E2.g:1	0.0093	-0.0009
927.9	E2.u:2	0	0	876.6	E2.g:2	0	0
1017.3	E1.g:1	0.0039	-0.0406	1005.2	E1.g:1	0.0064	-0.0406
1017.3	E1.g:2	0	0	1005.2	E1.g:2	0	0
1020.9	E1.u:1	0	0	1010	E1.u:1	0	0
1020.9	E1.u:2	0	0	1010	E1.u:2	0	0
1062.6	E2.u:1	0	0	1051.4	E2.u:1	0	0
1062.6	E2.u:2	0	0	1051.4	E2.u:2	0	0
1070.1	E2.g:1	0	0	1055.2	E2.g:1	0	0
1070.1	E2.g:2	0	-0.0023	1055.2	E2.g:2	0.0061	-0.0382
1133.8	A1.g	0.0001	0.0117	1128	A2.u	0	0
1135.1	A2.u	0	0	1129.6	A1.g	0.0002	-0.0202
1241.9	A2.g	0	-0.0001	1232.5	A2.g	0	0.0001
1242.3	A1.u	0	0	1232.8	A1.u	0	0
1388.2	E2.u:1	0	0	1397.9	E2.u:1	0	0
1388.2	E2.u:2	0	0	1397.9	E2.u:2	0	0
1401.2	E2.g:1	0	0.0070	1399.4	E2.g:1	0.0003	-0.0232
1401.2	E2.g:2	0	0	1399.4	E2.g:2		0
1432	E1.u:1	0	0	1424.2	E1.u:1	0	0
1432	E1.u:2	0	0	1424.2	E1.u:2	0	0
1435.6	E1.g:1	0	0	1427.7	E1.g:1	0	0
1435.6	E1.g:2	0.0013	0.0728	1427.7	E1.g:2	0.0015	-0.0680
3200.7	E2.u:1	0	0	3172.9	E2.u:1	0	0
3200.7	E2.u:2	0	0	3172.9	E2.u:2	0	0
3201.5	E2.g:1	0	0	3173.1	E2.g:1	0	0.0358
3201.5	E2.g:2	0	0.0022	3173.1	E2.g:2	0	0
3215.2	E1.g:1	0	0	3189.5	E1.g:1	0	0
3215.2	E1.g:2	0	0.0119	3189.5	E1.g:2	0	0.0130
3216.1	E1.u:1	0	0	3190.1	E1.u:1	0	0
3216.1	E1.u:2	0	0	3190.1	E1.u:2	0	0
3228.4	A2.u	0	0	3203	A2.u	0	0
3228.7	A1.g	0	-0.0009	3203.4	A1.g	0	-0.0089

References

1. Baerends, E. J.; Autschbach, J.; Berces, A.; Bo, C.; Boerrigter, P. M.; Cavallo, L.; Chong, D. P.; Deng, L.; Dickson, R. M.; Ellis, D. E.; Fan, L.; Fischer, T. H.; Fonseca Guerra, C.; van Gisbergen, S. J. A.; Groeneveld, J. A.; Gritsenko, O. V.; Grüning, M.; Harris, F. E.; van den Hoek, P.; Jacobsen, H.; van Kessel, G.; Kootstra, F.; van Lenthe, E.; Osinga, V. P.; Patchkovskii, S.; Philipsen, P. H. T.; Post, D.; Pye, C. C.; Ravenek, W.; Ros, P.; Schipper, P. R. T.; Schreckenbach, G.; Snijders, J. G.; Solà, M.; Swart, M.; Swerhone, D.; te Velde, G.; Vernooijs, P.; Versluis, L.; Visser, O.; van Wezenbeek, E.; Wiesenekker, G.; Wolff, S. K.; Woo, T. K.; Ziegler, T. *Adf 2003.01*, SCM: Amsterdam, 2003.

2. te Velde, G.; Bickelhaupt, F. M.; Baerends, E. J.; Fonseca Guerra, C.; van Gisbergen, S. J. A.; Snijders, J. G.; Ziegler, T., Chemistry with Adf. *Journal of Computational Chemistry* **2001**, *22*, 931-967.

3. van Lenthe, E.; Baerends, E. J., Optimized Slater-Type Basis Sets for the Elements 1–118. *Journal of Computational Chemistry* **2003**, *24*, 1142-1156.

4. Swart, M.; Bickelhaupt, F. M., Quild: Quantum-Regions Interconnected by Local Descriptions. *Journal of Computational Chemistry* **2008**, *29*, 724-734.

5. Swart, M.; Bickelhaupt, F. M., Optimization of Strong and Weak Coordinates. *International Journal of Quantum Chemistry* **2006**, *106*, 2536-2544.

6. Swart, M., Accurate Spin-State Energies for Iron Complexes. *Journal of Chemical Theory and Computation* **2008**, *4*, 2057–2066.

7. Swart, M.; Ehlers, A. W.; Lammertsma, K., The Performance of Opbe. *Molecular Physics* **2004**, *102*, 2467-2474.

8. Perić, M.; García-Fuente, A.; Zlatar, M.; Daul, C.; Stepanović, S.; García-Fernández, P.; Gruden-Pavlović, M., Magnetic Anisotropy in "Scorpionate" First-Row Transition-Metal Complexes: A Theoretical Investigation. *Chemistry – A European Journal* **2015**, *21*, 3716-3726.

9. Zlatar, M.; Gruden-Pavlović, M.; Schläpfer, C.-W.; Daul, C., Intrinsic Distortion Path in the Analysis of the Jahn–Teller Effect. *Journal of Molecular Structure: THEOCHEM* **2010**, *954*, 86-93.

10. Zlatar, M.; Schläpfer, C.-W.; Penka Fowe, E.; Daul Claude, A., Density Functional Theory Study of the Jahn-Teller Effect in Cobaltocene. *Pure and Applied Chemistry* 2009, 81, 1397–1411.

11. Ramanantoanina, H.; Zlatar, M.; García-Fernández, P.; Daul, C.; Gruden-Pavlović, M., General Treatment of the Multimode Jahn–Teller Effect: Study of Fullerene Cations. *Physical Chemistry Chemical Physics* **2013**, *15*, 1252-1259.

12. Neese, F., Prediction of Molecular Properties and Molecular Spectroscopy with Density Functional Theory: From Fundamental Theory to Exchange-Coupling. *Coordination Chemistry Reviews* **2009**, *253*, 526-563.

13. Phillips, J. J.; Peralta, J. E., Magnetic Exchange Couplings from Noncollinear Perturbation Theory: Dinuclear Cuii Complexes. *The Journal of Physical Chemistry A* **2014**, *118*, 5841-5847.

14. García, V. M.; Castell, O.; Caballol, R.; Malrieu, J. P., An Iterative Difference-Dedicated Configuration Interaction. Proposal and Test Studies. *Chemical Physics Letters* **1995**, *238*, 222-229.

15. Helgaker, T.; Jorgensen, P.; Olsen, J., *Molecular Electronic-Structure Theory*. Wiley: 2008.

16. Noodleman, L., Valence Bond Description of Antiferromagnetic Coupling in Transition Metal Dimers. *The Journal of Chemical Physics* **1981**, *74*, 5737-5743.

17. Noodleman, L.; Baerends, E. J., Electronic Structure, Magnetic Properties, Esr, and Optical Spectra for 2-Iron Ferredoxin Models by Lcao-X.Alpha. Valence Bond Theory. *Journal of the American Chemical Society* **1984**, *106*, 2316-2327.

18. Head-Gordon, M., Characterizing Unpaired Electrons from the One-Particle Density Matrix. *Chemical Physics Letters* **2003**, *372*, 508-511.

19. Staroverov, V. N.; Davidson, E. R., Distribution of Effectively Unpaired Electrons. *Chemical Physics Letters* **2000**, *330*, 161-168.

20. Neese, F., Definition of Corresponding Orbitals and the Diradical Character in Broken Symmetry Dft Calculations on Spin Coupled Systems. *Journal of Physics and Chemistry of Solids* **2004**, *65*, 781-785.

21. Soda, T.; Kitagawa, Y.; Onishi, T.; Takano, Y.; Shigeta, Y.; Nagao, H.; Yoshioka, Y.; Yamaguchi, K., Ab Initio Computations of Effective Exchange Integrals for H–H, H–He–H and Mn2o2 Complex: Comparison of Broken-Symmetry Approaches. *Chemical Physics Letters* **2000**, *319*, 223-230.

22. Haaland, A., The Molecular Structure of High-Spin Manganocene, (N-C5h5)2mn, by Gas Phase Electron Diffraction: A Rerefinement. *Inorganic and Nuclear Chemistry Letters* **1979**, *15*, 267-269.